Heliyon 10 (2024) e28495

Contents lists available at ScienceDirect

Heliyon

journal homepage: www.cell.com/heliyon

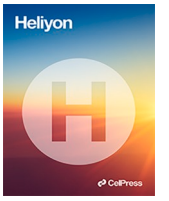

Research article

Design, synthesis, and evaluation of purine and pyrimidine-based *KRAS* G12D inhibitors: Towards potential anticancer therapy

So-Youn Park [a,1], Venu Venkatarame Gowda Saralamma [b,1], Sagar Dattatraya Nale [c], Chang Joong Kim [d], Yun Seong Jo [b], Mohammad Hassan Baig [b,*], JungHwan Cho [a,**]

[a] College of Pharmacy and Drug Information Research Institute, Sookmyung Women's University, 100 Cheongpa-ro 47-gil, Yongsan-gu, Seoul, 04310, Republic of Korea
[b] Department of Family Medicine, Yonsei University College of Medicine, Gangnam Severance Hospital, 211 Eonju-Ro, Gangnam-Gu, Seoul 06273, Republic of Korea
[c] BNJBiopharma, 2nd Floor Memorial Hall, 85, Songdogwahak-ro, Yeonsu-gu, Incheon 21983, Republic of Korea
[d] Department of Biotechnology, Graduate School, The Catholic University of Korea, Bucheon, Gyeonggi-do 14662, Republic of Korea

ARTICLE INFO

Keywords:
KRAS G12D
Anticancer
Inhibitors
Purine
Pyrimidine

ABSTRACT

Oncogenic *RAS* mutations, commonly observed in human tumors, affect approximately 30% of cancer cases and pose a significant challenge for effective cancer treatment. Current strategies to inhibit the *KRAS* G12D mutation have shown limited success, emphasizing the urgent need for new therapeutic approaches. In this study, we designed and synthesized several purine and pyrimidine analogs as inhibitors for the *KRAS* G12D mutation. Our synthesized compounds demonstrated potent anticancer activity against cell lines with the *KRAS* G12D mutation, effectively impeding their growth. They also exhibited low toxicity in normal cells, indicating their selective action against cancer cells harboring the *KRAS* G12D mutation. Notably, the lead compound, PU1-1 induced the programmed cell death of *KRAS* G12D-mutated cells and reduced the levels of active *KRAS* and its downstream signaling proteins. Moreover, PU1-1 significantly shrunk the tumor size in a pancreatic xenograft model induced by the *KRAS* G12D mutation, further validating its potential as a therapeutic agent. These findings highlight the potential of purine-based *KRAS* G12D inhibitors as candidates for targeted cancer therapy. However, further exploration and optimization of these compounds are essential to meet the unmet clinical needs of patients with *KRAS*-mutant cancers.

1. Introduction

The development of effective cancer therapies remains a difficult challenge in modern medicine. Although significant advancements have been made in this field, rat sarcoma (*RAS*) mutations present a major obstacle for treatment [1]. Canonical *RAS* genes include Kirsten-RAS (*KRAS*), neuroblastoma-RAS (*NRAS*), and Harvey-RAS (*HRAS*) [1]. *RAS* signaling pathways and their downstream

* Corresponding author. Department of Family Medicine, Yonsei University College of Medicine, Gangnam Severance Hospital, 211 Eonju-Ro, Gangnam-Gu, Seoul 06273, Republic of Korea
** Corresponding author. College of Pharmacy and Drug Information Research Institute, Sookmyung Women's University, Seoul, Republic of Korea.
E-mail addresses: mhbaig@yonsei.ac.kr (M.H. Baig), jcho@sookmyung.ac.kr (J. Cho).
[1] Authors sharing equal contribution.

https://doi.org/10.1016/j.heliyon.2024.e28495
Received 16 July 2023; Received in revised form 19 March 2024; Accepted 20 March 2024
Available online 2 April 2024

effectors control various cellular activities, including cell proliferation, survival, growth, metabolism, and migration [2,3]. RAS activity is governed by its switch-like behavior, transitioning between the active (GTP-bound) and inactive (GDP-bound) states [4]. However, mutations in *RAS*, particularly *KRAS*, lead to constitutive activation, resulting in the aberrant activation of the mitogen-activated protein kinase signaling pathway and subsequently contributing to cancer development and progression [4]. The first identification of oncogenic *RAS* mutations in human cancers in 1982 revolutionized our understanding of tumor formation and progression and established *RAS* as a critical driver of cancer [5,6]. *KRAS* is one of the most commonly mutated oncogene observed in solid tumors, particularly in colorectal cancer, lung adenocarcinoma, and pancreatic ductal adenocarcinoma (PDAC) [7]. Approximately 95% of cancer-associated RAS mutations occur at codons 12 (83%), 13 (14%), and 61 (2%). Among these, mutations at the glycine residue 12 (G12) of *KRAS* are the most common, followed by those at glycine residue 13 (G13) in *KRAS*. Moreover, G12C, G12V, and G12D are the most common substitutions in recurrent *KRAS* codon 12 mutations [1].

In recent years, significant advancements have been made in targeting *KRAS* mutations, which is regarded as the “holy grail" of targeted cancer therapies [8]. In 2013, a breakthrough was achieved in understanding *KRAS* biology, and advancements in drug design technologies revealed a cysteine drug-binding pocket in the GDP-bound mutant *KRAS* G12C protein [9]. This key finding facilitated the development of covalent inhibitors selectively targeting mutant *KRAS* G12C. Sotorasib (AMG510) and adagrasib (MRTX849) were the first and second U.S. Food and Drug Administration-approved selective and covalent *KRAS* G12C inhibitors, marking a significant milestone. Several other promising inhibitors (BPI-421286, JAB-21822, D-1553, GFH925, and GH35) are currently being developed [10]; however, effective *KRAS*-targeting drugs need to be developed. The *KRAS* G12D mutation is commonly observed in several cancers, including pancreatic, colon, and lung cancers, and poses a significant challenge for targeted cancer therapy [7,11]. This mutation is difficult to target because of the smooth surface and lack of suitable binding pockets. In PDAC, more than 90% of cases carry oncogenic *KRAS* mutations, with *KRAS* G12D being the most common variant. It is a major initiating mutation in a substantial proportion (45%) of PDAC cases, whose presence is associated with poor patient survival [12]. Currently, no therapeutic drugs targeting the *KRAS* G12D mutation have been approved for clinical use [12].

However, recent studies have revealed the benefits of targeting specific mutations in *KRAS* beyond the well-known hotspot variants. A remarkable breakthrough in this field was the pioneering work of Mirati Therapeutics. Using advanced structure-based drug design approaches, they successfully developed a novel non-covalent inhibitor, MRTX1133, specifically tailored to target the *KRAS* G12D mutation [1,11,13,14]. This inhibitor has demonstrated remarkable efficacy in preclinical studies, particularly in PDAC cells harboring the *KRAS* G12D mutation. These findings can aid in the development of effective therapeutic interventions for patients with *KRAS* G12D-driven cancers, offering a potential breakthrough in cancer treatment [11,13]. Previous studies on *KRAS* G12C inhibitors have revealed chemoresistance as the leading cause of treatment failure in *KRAS*-induced cancers [15–17]. Most patients do not respond to *KRAS* inhibitor therapy, owing to intrinsic or acquired resistance [18].

Purine- and pyrimidine-based molecules are widely used for anticancer drug development [19–21]. Several purine- and pyrimidine-based anticancer molecules have been successfully developed. For example, 5-fluorouracil (5-FU), a pyrimidine analog being used as an anticancer drug, inhibits thymidylate synthase, an enzyme involved in DNA synthesis, leading to impaired DNA replication and cell death [22,23]. It is used to treat various solid tumors, including colorectal, breast, and gastric cancers [24,25]. Mercaptopurine, fludarabine, cladribine, cytarabine, and gemcitabine are some well-known purine- and pyrimidine-based analogs used in anticancer research [20].

Bioisosteric methods involve the replacement of a part of a biologically active compound with other fragments [26–28]. This is a widely used approach for drug discovery. In this study we used a bioisosteric replacement method to design a series of novel purine and pyrimidine analogs as *KRAS* G12D inhibitors. The designed structures were synthesized, and their ability to inhibit the *KRAS* G12D mutation was tested using different *in vitro* methods. Several *in vitro* experimental assays, including the cell viability, apoptotic, and glutathione *S*-transferase-fused RBD (GST-RBD) pull-down assays were performed to evaluate the anticancer potential of the selected compounds in *KRAS* G12D-expressing cancer cells. The most active compound, PU1-1, was further evaluated *in vivo* in a *KRAS* G12D-induced pancreatic xenograft model.

2. Experimental section

2.1. Synthesis

The synthesis procedure for the new *KRAS* G12D derivatives, PU1-1, PU1-2, and PY (1–4), is depicted in Scheme 1 (Supplementary Material).

Commercially available 2-methyl-6-chloropurine was treated with benzyl bromide in the presence of K2CO3 to produce 9-benzyl-6-chloro-9H-purin-2-amine. The alkylated purine was treated with NaH to yield N,N, 9-tribenzyl-6-chloro-9H-purin-2-amine. Nucleophilic substitution of the secondary amine yielded urine derivatives, followed by deprotection of the *N*-Boc group using 4 N HCl to obtain the desired final compounds, PU1-1 and PU1-2, with a *KRAS* G12D warhead functional group.

The synthesis procedure of pyrimidine derivatives is outlined in Scheme 2 (Supplementary Material). Commercially available amidine with β-ketoester under the basic condition gave 4-oxopyrimides, followed by chlorination with phosphorous oxychloride to yield 4-chloropyrimidnes. The resulting 4-chloropyrimidines underwent nucleophilic substitution with a secondary amine to yield the corresponding pyrimidine derivatives, followed by deprotection of the *N*-Boc group using 4 N HCl or TFA to obtain the desired final compounds, PY1-1, PY1-2, and PY1-3. The detailed experimental procedures and characteristics of all new compounds are provided in the Supplementary Information.

2.2. Cell lines, reagents and antibodies

AGS (gastric cancer), MKN1 (gastric cancer), SNU1197 (colon cancer), AsPC1 (pancreatic cancer), PANC1 (pancreatic cancer), and Hek293 (normal kidney) cell lines were obtained from the Korean Cell Line Bank (Seoul, Korea). Antibiotics (penicillin/streptomycin), fetal bovine serum (FBS), and Roswell Park Memorial Institute (RPMI)-1640 cell culture growth medium were purchased from Gibco (Thermo Fisher Scientific). Bio-Rad Laboratories Inc. Provided the chemicals and materials used for electrophoresis. EZ-CYTOX cell viability, proliferation, and cytotoxicity assay kits were purchased from Do Gen Bio (Korea). Antibodies specific for ERK, pERK, S6, pS6, PARP, and *KRAS* were acquired from Cell Signaling Technology (Danvers, MA, USA). Santa Cruz provided the AKT and pAKT antibodies and β-actin.

2.3. Cell lines and culture

AGS, SNU1197, AsPC1, and MKN1 cells were cultured and maintained in the RPMI-1640 medium (Gibco, Life Technologies, Carlsbad, CA, USA). All experiments in this study were conducted using mycoplasma-free cell lines to ensure the accuracy and reliability of the results. The medium was supplemented with 1% penicillin–streptomycin (Gibco) and 10% FBS (Gibco). The cells were cultured at 37 °C with 5% CO_2 in a humidified environment. Similarly, PANC1 and Hek293 cell lines were cultured in the Dulbecco's modified Eagle's medium (Gibco) supplemented with 1% penicillin–streptomycin (Gibco) and 10% FBS (Gibco). These cells were also maintained at 37 °C with 5% CO_2 in a humidified environment.

2.4. WST cell viability assay

The viability of cancer cells was assessed using the WST cell viability assay, which utilizes the water-soluble tetrazolium salt method. To begin, cells were seeded in a 96-well plate at a density of 3000–5000 cells per well and allowed to grow overnight. Subsequently, the cells were subjected to different treatments: either a control (DMSO $\leq$1%) or various concentrations of new inhibitors, starting at 10 μM and diluted two-fold, for 72 h. To determine cell viability, the EZ-CyTox Cell Viability Assay Kit (manufactured by Daeil Lab Service Co., Ltd., Korea) was employed following the provided instructions. In brief, after the incubation period, the cells were supplemented with 10 μl of EZ-CyTox solution containing WST-1 (Water-Soluble Tetrazolium Salt) and incubated for 2 h. The absorbance was then measured at 450 nm using a GloMax® Discover microplate reader from Promega (WI, USA). Concurrently, wells containing only the medium without cells were incubated with 10 μl of EZ-CyTox solution to determine the background signal. The final cell viability percentage was calculated using the following formula: Cell viability (%) = $(A_{treatment})/(A_{control}) \times 100$ (%) where A = absorbance at 450 nm.

2.5. Apoptosis detection assay

Apoptotic cells were identified using a FITC Annexin-V apoptosis detection kit 1 obtained from BD Pharmingen in San Diego, CA, USA. In brief, AGS and MKN1 cells were seeded at a density of 3–5 $\times$ 10^5 cells/well in 6-well plates and incubated overnight. The cells were treated with PU1-1 at concentrations of 0, 2.5, and 5 μM for 24 h. After treatment, the cells were collected, washed with PBS, and resuspended in 1X binding buffer. Subsequently, the cells were stained with Annexin V-FITC and PI for 15 min at room temperature in the dark, and a binding buffer was added. Flow cytometry data were analyzed using the BD FACSAria™ III Cell Sorter flow cytometer.

2.6. Immunoblotting

AGS and MKN1 cells were seeded at a density of 3–5 $\times$ 10^5 cells/well in 6-well plates and allowed to grow overnight. The cells were treated with Dimethyl sulfoxide (DMSO) as a control or PU1-1 at 5 μM and 7.5 μM concentrations for 24 h. Following the treatment, the cells were washed once with 1x phosphate-buffered saline (PBS) and lysed in RIPA buffer obtained from iNtRON Biotechnology, supplemented with a cocktail of protease and phosphatase inhibitors from Thermo Scientific. The protein concentrations were determined using the Pierce BCA protein assay kit provided by Thermo Scientific. Equal amounts of protein were resolved on 8–12% SDS-PAGE and transferred onto nitrocellulose membranes. The membranes were blocked with 5% non-fat milk in TBST (Tris-buffered saline with Tween) and then incubated overnight at 4 °C with primary antibodies. After washing, the membranes were incubated with HRP-conjugated secondary antibodies for 1 h at room temperature. The blots were washed five times with TBS-T and developed using an Enhanced chemiluminescent (ECL) detection system obtained from EMD Millipore.

2.7. GST-RBD pulldown assay

AGS and MKN1 cells were treated with DMSO or PU1-1 (0, 5 and 7.5 μM) for 24 h and cell lysate prepared using 1X passive lysis buffer (Promega). A total of 400 μg protein in 500 μL total volume was pulled down using the Glutathione-GST-RBD (complex) overnight, and the pulldown proteins were detected by immunoblotting with *anti-KRAS* antibody.

2.8. In vivo antitumor efficacy study

All mouse experiments complied with the Institutional Animal Care and Use Committee regulations and guidelines of the Lee Gill

Ya Cancer and Diabetes Institute, Gachon University. Female BALB/c nude mice, aged 5–6 weeks, were obtained from ORIENT BIO, Inc. To establish a tumor model, AsPC1 tumor cells (5.0×10^6 cells) were subcutaneously injected into the right hind flank of each mouse in 100 μL of PBS. The mice were observed twice a week for two weeks, and tumor growth was monitored by measuring the tumor size using calipers when they became palpable. Once the tumors reached an average volume of >100 mm^3, the mice were randomly assigned to the following treatment groups: control and PU1-1. The animals received daily intraperitoneal injections of the vehicle or PU1-1. Daily monitoring of the mice, including tumor size measurements thrice per week and body weight measurements twice per week, was performed for 14 days. Tumor growth inhibition (TGI) was assessed using the following formula: 100% × (final vehicle tumor volume – final treated tumor volume/final vehicle tumor volume – initial vehicle tumor volume). The mice were euthanized in a CO_2 chamber, and the tumors were extracted for further study. TGI (%) was calculated using the following formula: TGI (%) = $(1 - [RTV_{treatment}]/[RTV_{control}]) \times 100$ (%). The relative tumor volume (RTV) was calculated using the following formula: RTV = tumor volume on the measured day/tumor volume on day 0.

2.9. In silico analysis

The designed compounds were subjected to various *in silico* analyses to gain insights into their binding to the active site of *KRAS* G12D. A molecular docking study was performed to determine the binding affinity of the designed compounds using Glide [29]. Further molecular dynamics simulation studies were conducted to understand the structural dynamics of the inhibitors bound to the active site of *KRAS* G12D. GROMACS version 2020.7. was used for MD simulations, as previously described [30–32]. CHARMM parameters were generated using the SwissParam web server [33]. The trajectory results were analyzed using the UCSF-chimera software, whereas plots were generated using the XMGRACE tool (https://plasma-gate.weizmann.ac.il/Grace/).

3. Results

3.1. Biological evaluations

3.1.1. In vitro assay: evaluating the inhibitors' effect on cancer cell viability

The effects of newly synthesized purine- and pyrimidine-based KRAS inhibitors on the viability of AGS, SNU1197, AsPC1, and Hek293 cells were determined by seeding them at 3000–5000 cells/well in a 96-well plate and culturing them overnight. All cells were treated with the control (DMSO ≤1%) or 2-fold dilution of purine- and pyrimidine-based KRAS inhibitors with a starting concentration of 10 μM for 72 h. After 72 h of incubation, cell viability was measured using the WST assay. The percentage of viable cells was plotted, and the IC50 was calculated using the GraphPad Prism software (http://www.graphpad.com/quickcalcs/ConfInterval1.cfm). As shown in Table 1, most compounds showed cell inhibition at IC50 < 10 μM. Specifically, PU1-1 inhibited all three KRAS G12D cell lines at an average IC50 of 4.4 μM. While it demonstrated IC50 of 9.2 μM in Hek293 cells, indicating its selective cytotoxicity toward cancer cells (Fig. 1 A and 1 B). Based on these results, we further evaluated the cell inhibitory effect of PU1-1 in a panel of cancer cells from different backgrounds (Fig. 1 A) and calculated the IC50 values. PU1-1 showed the most potent growth inhibition in all KRAS G12D mutant cell lines than in the KRAS wild-type (WT) MKN1 and normal (Hek293) cell lines, confirming its selectivity (Fig. 1 A and 1 B). Therefore, we selected PU1-1 for subsequent experiments.

3.1.2. PU1-1 induced KRAS G12D cell apoptosis

To assess whether PU1-1 induces cancer cell apoptosis, AGS and MKN1 cells were treated for 24 h at different PU1-1 concentrations (0, 2.5, and 5 μM), stained with Annexin V-FITC/PI, and analyzed via flow cytometry (BD FACSAria III Cell Sorter). As shown in Fig. 2, after 24 h treatment with different concentrations of PU1-1, the proportion of early (LR) and late apoptotic (UR) cells increased. These results confirmed that PU1-1 efficiently induces apoptosis in gastric cancer. MKN1 (KRAS wild-type) cells treated with PU1-1 (0, 2.5, and 5 μM) for 24 h did not show significant apoptosis, indicating the specificity of the inhibitor toward KRAS G12D-induced cancers. These results confirmed that PU1-1 efficiently induces apoptosis in KRAS G12D-mutated cells.

3.1.3. PU1-1 reduces active-KRAS protein along with its downstream proteins in KRAS G12D mutant cells

To investigate whether PU1-1 inhibits the active form of *KRAS* (GTP bound), GST-RBD pull-down assay followed by western blotting analysis was performed in 24 h PU1-1 (5 or 7.5 μM) treated AGS and MKN1 cells. Indeed, PU1-1 significantly downregulated

Table 1
In vitro antiproliferative activity of compounds.

ID	IC50 (μM)			
	AGS (G12D)	AsPC1 (G12D)	SNU1197 (G12D)	Hek293 (Normal)
PY1-1	9.1 ± 1.4	6.4 ± 0.2	N/A	4.5 ± 0.3
PY1-2	3.3 ± 0.6	10.9 ± 0.4	N/A	9.1 ± 0.7
PU1-1	3.2 ± 0.4	5.9 ± 0.3	3.8 ± 0.8	9.2 ± 0.2
PU1-2	3.5 ± 0.7	6.3 ± 0.7	2.9 ± 0.3	5.6 ± 0.2
PY1-3	6.5 ± 1.2	5.8 ± 0.2	7 ± 0.6	4.5 ± 0.4
MRTX1133	0.0065	0.062	0.037	19.69

A

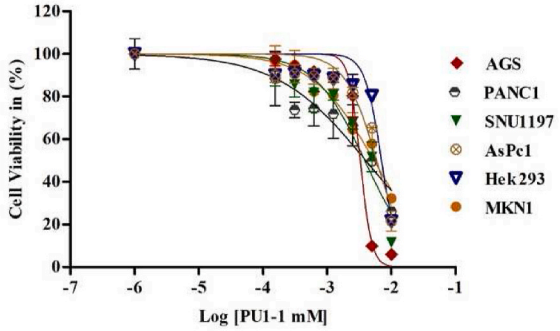

B

Sr. No.	Cell line	IC50 (μM)
1	AGS (G12D)	3.2 ±0.4
2	PANC1 (G12D)	3.9±0.7
3	SNU1197 (G12D)	3.8±0.8
4	AsPc1 (G12D)	5.9±0.3
5	Hek293 (Normal)	9.2±0.2
6	MKN1 (WT)	5.3±0.4

Fig. 1. Effect of PU1-1 on the cell viability of different cancer cells: **(A).** Different cancer cells, AGS, SNU1197, PANC1, AsPC1, MKN1 and Hek293 cells were seeded at 3000–5000 cells per well in 96 well plate and grown overnight. All the cells were treated with either Control (DMSO 1%) or with 2-fold dilution of PU1-1 with a starting concentration of 10,000 nM for 72 h. After 72 h incubation, cell viability was measured using WST assay. The IC50 values were calculated using GraphPad Prism and listed. **(B).** Data are presented as the mean ± SD. Each *KRAS* G12D cell sample was measured three times separately.

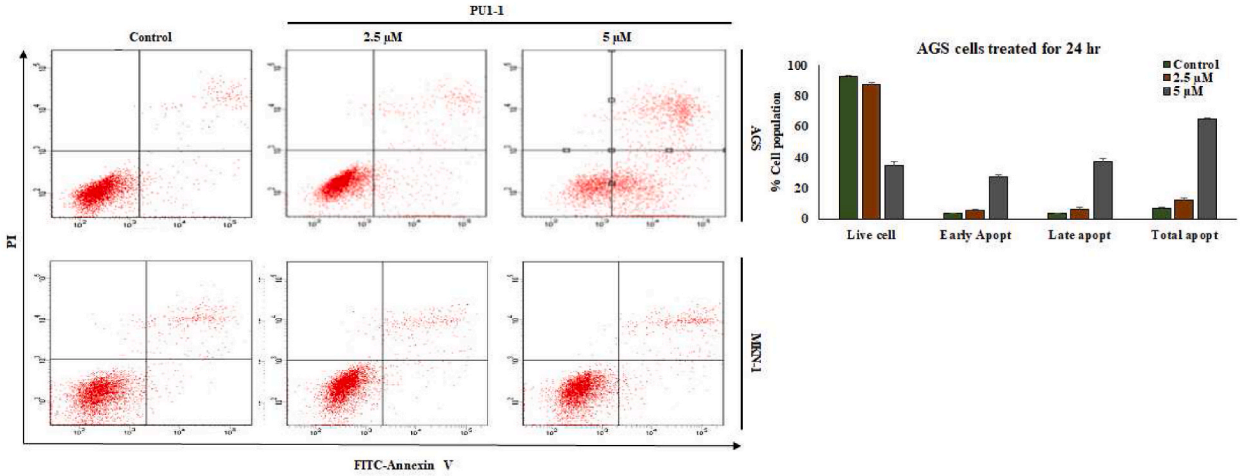

Fig. 2. To assess whether PU1-1 could induce cancer cell apoptosis, AGS and MKN1 were treated with PU1-1 at different concentrations (0, 2.5, and 5 μM) for 24 h and stained with Annexin V-FITC/PI and analyzed by flow cytometry (BD FACSAria™ III Cell Sorter).

the KRAS-GTP levels in AGS cells in a dose-dependent manner (Fig. 3A). To further understand its mechanism of action, we evaluated the effects of PU1-1 on the downstream signals of *KRAS*. PU1-1 treatment significantly decreased the pERK, pAKT, and pS6 levels in a dose-dependent manner. As PU1-1 induced apoptotic cell death in AGS cells, we examined the apoptotic markers, PARP and cleaved PARP in these cells. PU1-1 significantly increased the levels of cleaved PARP in the drug-treated groups than in the DMSO-treated group, indicating that PU1-1 induces apoptosis in AGS cells (Fig. 3C). While in the *KRAS* wild-type (MKN1 cells), PU1-1 showed no protein expression changes in KRAS-GTP and *KRAS* downstream proteins, including PARP (Fig. 3B and D). These results suggest that PU1-1 specifically reduces the active *KRAS* levels in *KRAS* G12D cells by inducing dose-dependent apoptotic cell death.

3.2. PU1-1 suppresses tumor growth in the KRAS G12D-induced pancreatic xenograft model

To assess the *in vivo* antitumor activity of PU1-1, an AsPC1 female BALB/c mouse model was established. After attaining the tumor volume ≥100 mm^3, mice were treated with the vehicle control (40% PEG300 + 10% DMSO + 5% Tween-80 + 45% saline: in 200 μL/mouse) or PU1-1 (15 mg/kg 10% DMSO + 5% Tween-80 + 40% PEG300 + 45% saline: in 200 μL/mouse) were administered intraperitoneal (i.p.) once daily for 14 days. As shown in Fig. 4A. PU1-1 suppressed AsPC1 tumor growth, with a TGI of 42% on day 14. Therefore, PU1-1 is a promising *KRAS* G12D inhibitor that warrants further investigation as a potential anticancer agent. The mice showed no noticeable weight loss during treatment (Fig. 4B).

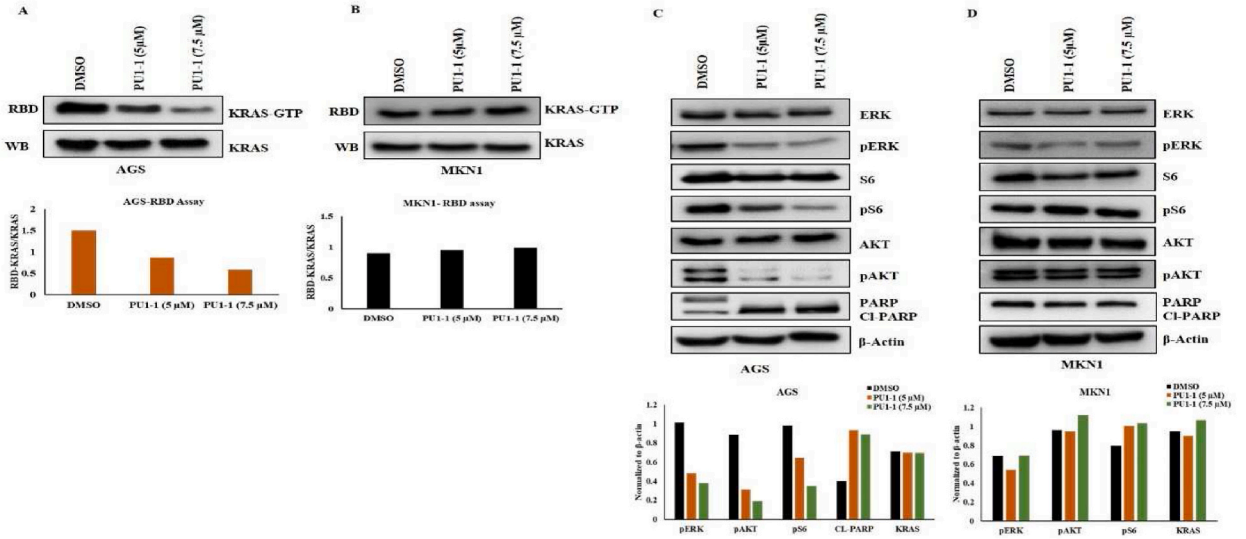

Fig. 3. Effect of PU1-1 on the Active-*KRAS* protein in AGS and MKN1 cells were analyzed using GST-RBD pulldown assay: (A, B): Effect of PU1-1 on the Active-*KRAS* protein in AGS and MKN1 cells were analyzed using GST-RBD pulldown assay and representative band intensity was quantified (n = 2). **(C,D):** The intensity of the bands in (c) and (d) was quantified and normalized to the expression of loading control (β-actin) (n = 2) (RBD: RBD pulldown sample, WB: Western blot of cell lysate).

3.3. *In silico analysis*

Molecular docking studies are widely used for hit identification and lead optimization, in which small molecules are "docked" against macromolecular targets, which are further ranked based on their binding affinities [34–37]. A molecular docking simulation study was conducted to better understand the interaction of these compounds within the SWII-binding site of the *KRAS* G12D protein (PDB code: 7RPZ). PU1-2 was found to effectively bind within the active site of *KRAS* G12D with a binding affinity of −4.855 Kcal/mol, followed by PU1-1 which showed a binding affinity of −4.565 Kcal/mol (Table 2). Molecular docking revealed that purine-based compounds were more effective in binding to *KRAS* G12D than their pyrimidine counterparts. As shown in Fig. 5, all compounds shared similar binding conformations within the binding site of *KRAS* G12D and the same pocket as MRTX1133. Moreover, hydrophobic interactions governed the binding of all compounds.

Molecules complex with *KRAS* G12D were subjected to MD-based studies using the GROMACS software package. MD simulation is a principal tool for drug discovery to investigate the structural changes within proteins, DNA, or any other biological molecules and their complexes [35,38,39]. This study provides insight into the binding of these compounds with the active site of *KRAS* G12D. We observed the ligand root mean square deviation (RMSD), which measures the deviation of the ligand from the active site during the

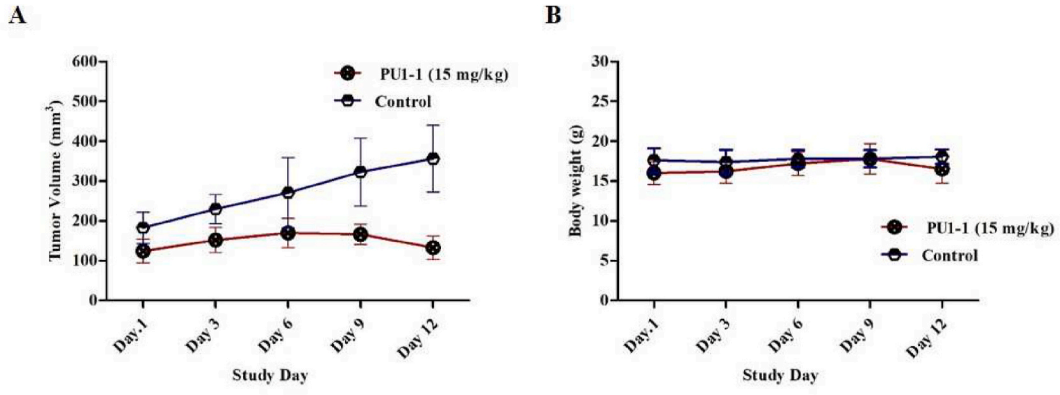

Fig. 4. To assess the *in vivo* antitumor activity of compound PU1-1, an AsPC1 female BALB/c mice model was established. After the tumor volume reached approximately ≥100 mm^3, mice were treated either with vehicle control (10 % DMSO+ 40% PEG300 + 5% Tween-80 + 45% saline: in 200 μl/mouse) or PU1-1 (15 mg/kg10% DMSO+40% PEG300 + 5% Tween-80 + 45% saline: in 200 μl/mouse), by intraperitoneal (i.p.) injection once a day for 14 days. PU1-1 compounds suppressed AsPC1 tumor growth with a TGI (tumor growth inhibition) of 42% **(A).** Changes in the body weight **(B).**

Table 2
Binding affinities of the selected compounds against *KRAS* G12D.

Sr. No.	Compounds	Glide Docking Score (Kcal/mol)
1.	**PY1-1**	−3.860
2.	**PY1-2**	−3.898
3.	**PU1-1**	−4.565
4.	**PU1-2**	−4.855
5.	**PY1-3**	−3.451

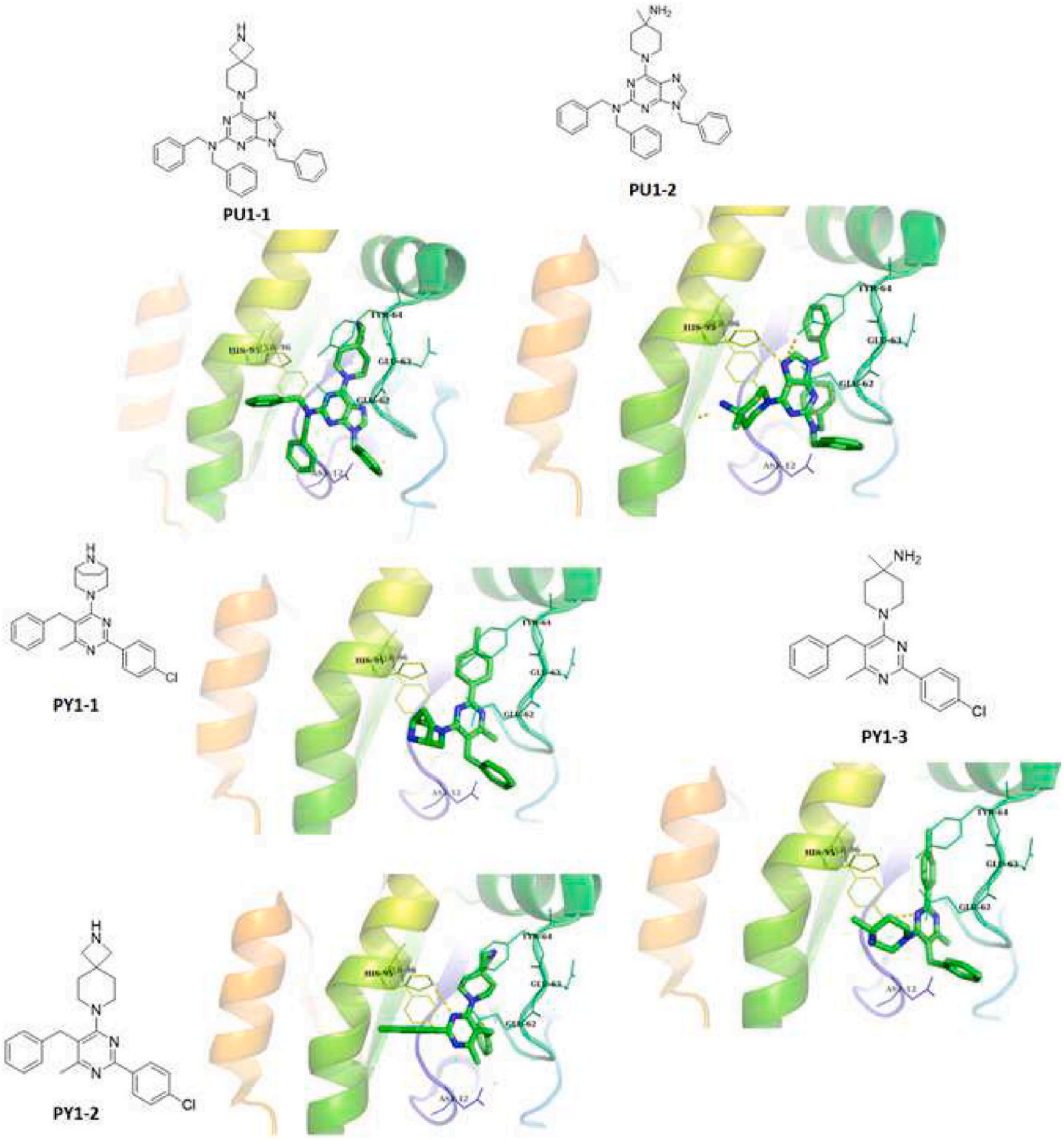

Fig. 5. The structure of all the compounds shortlisted in this study and their binding orientation within the active site of *KRAS* G12D.

simulation. This is another measure for monitoring the binding stability of any compound within the protein-binding pocket. Most molecules had stable RMSD plots and deviations of less than 3 Å, as shown in Fig. 6A. Initially, PU1-1 exhibited some RMS fluctuation, which later stabilized (below 3Å) for the remaining time period. Notably, *in silico* findings do not always corroborate the experimental results. *In silico* results are a valuable tool in scientific research; however, they may not always correlate perfectly with the experimental results [40]. In this study, *in silico* analysis was performed to gain further insight into the binding of molecules to the active site of *KRAS* G12D. Hydrogen bonds play a vital role in the overall stability of the protein–ligand complexes [41]. In addition, we analyzed the hydrogen bond formation for 200 ns. Analysis of H-bonds is another method to determine the binding capability of any compound.

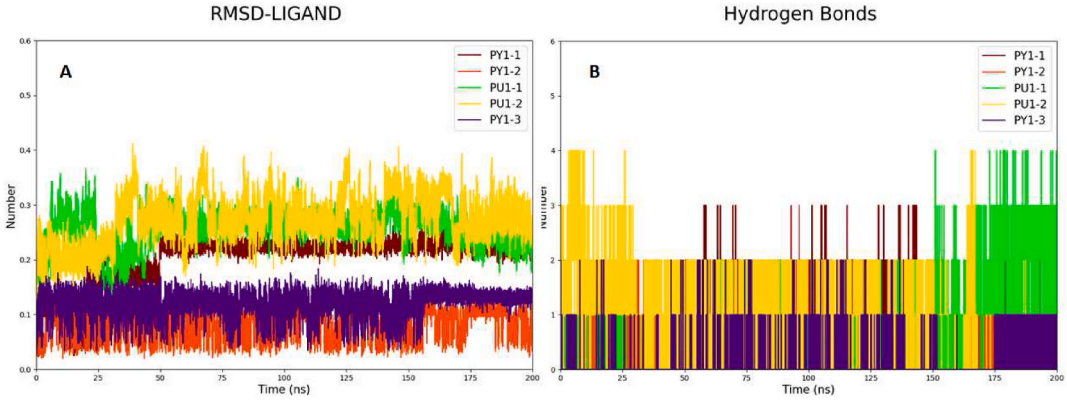

Fig. 6. The image indicates (a) the RMSD plots and (b) hydrogen bond plots of the selected molecules.

The higher the number of hydrogen bonds, the more stable the complex. The selected molecules exhibited an average of three hydrogen bonds throughout the simulation (Fig. 6B).

4. Discussion and conclusion

Recent advancements in the understanding of KRAS biology and the development of innovative drug design strategies have provided new targeted therapies for KRAS-mutated malignancies [14,42–45]. These breakthroughs have led to significant progress in overcoming the challenges associated with KRAS mutation-induced disease treatment [30,31,33]. This progress has tremendous potential for transforming the treatment landscape for patients with KRAS-driven cancers [44,32]. Nevertheless, much remains to be discovered as most small GTPases and hotspot mutations remain unexplored. Additionally, the emergence of clinical resistance to G12C inhibitors presents new challenges in cancer treatment [15–17]. Nonetheless, these advancements indicate exciting possibilities for KRAS-targeted therapies [46].

Despite recent progress in the development of KRAS G12D inhibitors, several challenges remain. A major challenge in targeting the KRAS G12D mutation is achieving sufficient selectivity for mutant KRAS while preventing the inhibition of wild-type KRAS that plays an essential role in normal cellular signaling [46–48]. Another challenge is ensuring adequate drug delivery to the tumor tissues [49]. Moreover, KRAS G12D inhibitors may be toxic and drug-resistant. A multidisciplinary approach involving collaboration among medicinal chemists, pharmacologists, and oncologists is necessary to overcome these challenges [10]. Recent advances in medicinal chemistry have led to the development of various KRAS G12C inhibitors, such as sotorasib and adagrasib, which show efficacy in treating various G12C harboring cancers [50,51]. However, the lack of an approved small-molecule drug for the KRAS G12D mutation highlights the need to develop selective inhibitors targeting this KRAS variant.

Design and synthesis of small-molecule inhibitors is one of the most promising approaches for the development of KRAS mutation-targeting therapies. Various inhibitors have been designed to specifically bind to mutated KRAS proteins and prevent downstream signaling pathways that lead to tumor growth [8]. One approach involves the development of purine-based KRAS G12D inhibitors. These inhibitors are specifically designed to target the KRAS G12D mutation, which is one of the most common and aggressive mutations found in several cancers, including pancreatic cancer.

In this study, we developed and synthesized a series of novel analogs based on purine and pyrimidine structures to design effective *KRAS* G12D inhibitors. Our developed compounds exhibited potent antiproliferative activity in cancer cell lines carrying the *KRAS* G12D mutation (AGS, SNU1197, and AsPC1) with IC50 values in the low micromolar range. Among the tested analogs, PU1-1 consistently exhibited significant anti-proliferative activity, with an average IC50 of 3.6 μM in three *KRAS* G12D-mutated cell lines (AGS, SNU1197, and PANC1). It was observed that the purine-based compounds were more effective on AGS and SNU1197 cell lines, while they showed higher IC50 on the AsPC1 cells. In contrast, pyrimidine-based compounds were comparatively less effective on all the studied cell lines. Except for PY1-2, which showed an IC50 of 3.3 μM on the AGS cells, other molecules in this class were not found to be very effective (IC50 higher than the normal cells). The comparative analysis found that pyrimidine-based compounds showed lower IC50 on normal cells than cancer cells, making them unsuitable. At the same time, the purine-based compounds (PU1-1 and PU1-2) showed consistent anticancer potential, especially PU1-1. This compound was comparatively more selective against cancer cells than its normal counterpart. Further investigations revealed that PU1-1 effectively reduced the active form of KRAS (KRAS-GTP) in AGS (KRAS G12D harboring) cancer cells but not in KRAS wild-type harboring MKN1 cells. Additionally, PU1-1 induced apoptosis and downregulated phosphorylated ERK levels in AGS cancer cells but not in MKN1 cells. Interestingly, in an AsPC1 tumor model, treatment with PU1-1 (15 mg/kg) resulted in significant antitumor efficacy, with a TGI of 42%. These findings highlight the potential of PU1-1 as a promising KRAS G12D inhibitor and warrant its further optimization as an anticancer agent. In summary, our study outlines the design and synthesis of novel purine and pyrimidine analogs as potential KRAS G12D inhibitors. Here, PU1-1 exhibited potent antiproliferative activity, selective KRAS-GTP reduction, apoptosis induction, and phosphorylated ERK downregulation. Our results suggest the need for further optimization and exploration of PU1-1 as a potential therapeutic candidate for cancer.

5. Data availability statement

The datasets used and/or analyzed during the current study are available from the corresponding author on reasonable request.

CRediT authorship contribution statement

So-Youn Park: Writing – review & editing, Investigation. **Venu Venkatarame Gowda Saralamma:** Methodology, Investigation. **Sagar Dattatraya Nale:** Methodology. **Chang Joong Kim:** Methodology, Investigation. **Yun Seong Jo:** Methodology, Investigation. **Mohammad Hassan Baig:** Writing – original draft, Supervision, Conceptualization. **JungHwan Cho:** Writing – review & editing, Supervision, Conceptualization.

Declaration of competing interest

The authors declare that they have no known competing financial interests or personal relationships that could have appeared to influence the work reported in this paper.

Appendix A. Supplementary data

Supplementary data to this article can be found online at https://doi.org/10.1016/j.heliyon.2024.e28495.

References

[1] D. Wei, L. Wang, X. Zuo, A. Maitra, R.S. Bresalier, A small molecule with big impact: MRTX1133 targets the KRASG12D mutation in pancreatic cancer, Clin. Cancer Res. 30 (4) (2023) 655–662.
[2] R.C. Gimple, X. Wang, RAS: striking at the core of the oncogenic circuitry, Front. Oncol. 9 (2019) 965.
[3] K. Rajalingam, R. Schreck, U.R. Rapp, S. Albert, Ras oncogenes and their downstream targets, Biochim. Biophys. Acta 1773 (8) (2007) 1177–1195.
[4] L. Huang, Z. Guo, F. Wang, L. Fu, KRAS mutation: from undruggable to druggable in cancer, Signal Transduct. Targeted Ther. 6 (1) (2021) 386.
[5] A.K. Murugan, M. Grieco, N. Tsuchida, RAS mutations in human cancers: roles in precision medicine, Semin. Cancer Biol. 59 (2019) 23–35.
[6] J. Lv, J. Wang, S. Chang, M. Liu, X. Pang, The greedy nature of mutant RAS: a boon for drug discovery targeting cancer metabolism? Acta Biochim. Biophys. Sin. 48 (1) (2016) 17–26.
[7] Y. Yang, H. Zhang, S. Huang, Q. Chu, KRAS mutations in solid tumors: characteristics, current therapeutic strategy, and potential treatment exploration, J. Clin. Med. 12 (2) (2023).
[8] X. Zhou, Y. Ji, J. Zhou, Multiple strategies to develop small molecular KRAS directly bound inhibitors, Molecules 28 (8) (2023).
[9] J.M. Ostrem, U. Peters, M.L. Sos, J.A. Wells, K.M. Shokat, K-Ras(G12C) inhibitors allosterically control GTP affinity and effector interactions, Nature 503 (7477) (2013) 548–551.
[10] Z. Mao, H. Xiao, P. Shen, Y. Yang, J. Xue, Y. Yang, Y. Shang, L. Zhang, X. Li, Y. Zhang, Y. Du, C.C. Chen, R.T. Guo, Y. Zhang, KRAS(G12D) can be targeted by potent inhibitors via formation of salt bridge, Cell Discov 8 (1) (2022) 5.
[11] Q. He, Z. Liu, J. Wang, Targeting KRAS in PDAC: a new way to cure it? Cancers 14 (20) (2022).
[12] S.F. Bannoura, H.Y. Khan, A.S. Azmi, KRAS G12D targeted therapies for pancreatic cancer: has the fortress been conquered? Front. Oncol. 12 (2022) 1013902.
[13] X. Wang, S. Allen, J.F. Blake, V. Bowcut, D.M. Briere, A. Calinisan, J.R. Dahlke, J.B. Fell, J.P. Fischer, R.J. Gunn, J. Hallin, J. Laguer, J.D. Lawson, J. Medwid, B. Newhouse, P. Nguyen, J.M. O'Leary, P. Olson, S. Pajk, L. Rahbaek, M. Rodriguez, C.R. Smith, T.P. Tang, N.C. Thomas, D. Vanderpool, G.P. Vigers, J. G. Christensen, M.A. Marx, Identification of MRTX1133, a noncovalent, potent, and selective KRAS(G12D) inhibitor, J. Med. Chem. 65 (4) (2022) 3123–3133.
[14] A.L. Hansen, X. Xiang, C. Yuan, L. Bruschweiler-Li, R. Bruschweiler, Excited-state observation of active K-Ras reveals differential structural dynamics of wild-type versus oncogenic G12D and G12C mutants, Nat. Struct. Mol. Biol. 30 (10) (2023) 1446–1455.
[15] M.M. Awad, S. Liu, I.I. Rybkin, K.C. Arbour, J. Dilly, V.W. Zhu, M.L. Johnson, R.S. Heist, T. Patil, G.J. Riely, J.O. Jacobson, X. Yang, N.S. Persky, D.E. Root, K. E. Lowder, H. Feng, S.S. Zhang, K.M. Haigis, Y.P. Hung, L.M. Sholl, B.M. Wolpin, J. Wiese, J. Christiansen, J. Lee, A.B. Schrock, L.P. Lim, K. Garg, M. Li, L. D. Engstrom, L. Waters, J.D. Lawson, P. Olson, P. Lito, S.I. Ou, J.G. Christensen, P.A. Janne, A.J. Aguirre, Acquired resistance to KRAS(G12C) inhibition in cancer, N. Engl. J. Med. 384 (25) (2021) 2382–2393.
[16] A. Di Federico, I. Ricciotti, V. Favorito, S.V. Michelina, P. Scaparone, G. Metro, A. De Giglio, F. Pecci, G. Lamberti, C. Ambrogio, B. Ricciuti, Resistance to KRAS G12C inhibition in non-small cell lung cancer, Curr. Oncol. Rep. 25 (9) (2023) 1017–1029.
[17] N. Tanaka, J.J. Lin, C. Li, M.B. Ryan, J. Zhang, L.A. Kiedrowski, A.G. Michel, M.U. Syed, K.A. Fella, M. Sakhi, I. Baiev, D. Juric, J.F. Gainor, S.J. Klempner, J. K. Lennerz, G. Siravegna, L. Bar-Peled, A.N. Hata, R.S. Heist, R.B. Corcoran, Clinical acquired resistance to KRAS(G12C) inhibition through a novel KRAS switch-II pocket mutation and polyclonal alterations converging on RAS-MAPK reactivation, Cancer Discov. 11 (8) (2021) 1913–1922.
[18] J. Liu, R. Kang, D. Tang, The KRAS-G12C inhibitor: activity and resistance, Cancer Gene Ther. 29 (7) (2022) 875–878.
[19] D.J. Baillache, A. Unciti-Broceta, Recent developments in anticancer kinase inhibitors based on the pyrazolo[3,4-d]pyrimidine scaffold, RSC Med. Chem. 11 (10) (2020) 1112–1135.
[20] W.B. Parker, Enzymology of purine and pyrimidine antimetabolites used in the treatment of cancer, Chem Rev 109 (7) (2009) 2880–2893.
[21] B. Tylinska, B. Wiatrak, Z. Czyznikowska, A. Ciesla-Niechwiadowicz, E. Gebarowska, A. Janicka-Klos, Novel pyrimidine derivatives as potential anticancer agents: synthesis, biological evaluation and molecular docking study, Int. J. Mol. Sci. 22 (8) (2021).
[22] N. Zhang, Y. Yin, S.J. Xu, W.S. Chen, 5-Fluorouracil: mechanisms of resistance and reversal strategies, Molecules 13 (8) (2008) 1551–1569.
[23] J. Wang, M. Yang, S. Yagi, R.M. Hoffman, Oral 5-FU is a more effective antimetastatic agent than UFT, Anticancer Res. 24 (3a) (2004) 1353–1360.
[24] H. Wilke, M. Stahl, W. Koster, U. Vanhofer, [Infusiontherapy with 5-fluorouracil ("infusional" 5-FU) in solid tumors], Med. Klin. 95 (Suppl 1) (2000) 3–8.
[25] K. Miura, M. Kinouchi, K. Ishida, W. Fujibuchi, T. Naitoh, H. Ogawa, T. Ando, N. Yazaki, K. Watanabe, S. Haneda, C. Shibata, I. Sasaki, 5-fu metabolism in cancer and orally-administrable 5-fu drugs, Cancers 2 (3) (2010) 1717–1730.
[26] G. Maggiora, M. Vogt, D. Stumpfe, J. Bajorath, Molecular similarity in medicinal chemistry, J. Med. Chem. 57 (8) (2014) 3186–3204.
[27] S.R. Langdon, P. Ertl, N. Brown, Bioisosteric replacement and scaffold hopping in lead generation and optimization, Mol Inform 29 (5) (2010) 366–385.
[28] A. Dick, S. Cocklin, Bioisosteric replacement as a tool in anti-HIV drug design, Pharmaceuticals 13 (3) (2020).
[29] R.A. Friesner, R.B. Murphy, M.P. Repasky, L.L. Frye, J.R. Greenwood, T.A. Halgren, P.C. Sanschagrin, D.T. Mainz, Extra precision glide: docking and scoring incorporating a model of hydrophobic enclosure for protein-ligand complexes, J. Med. Chem. 49 (21) (2006) 6177–6196.

[30] S.B. Kemp, N. Cheng, N. Markosyan, R. Sor, I.K. Kim, J. Hallin, J. Shoush, L. Quinones, N.V. Brown, J.B. Bassett, N. Joshi, S. Yuan, M. Smith, W.P. Vostrejs, K. Z. Perez-Vale, B. Kahn, F. Mo, T.R. Donahue, C.G. Radu, C. Clendenin, J.G. Christensen, R.H. Vonderheide, B.Z. Stanger, Efficacy of a small-molecule inhibitor of KrasG12D in immunocompetent models of pancreatic cancer, Cancer Discov. 13 (2) (2023) 298–311.
[31] D.S. Hong, M.G. Fakih, J.H. Strickler, J. Desai, G.A. Durm, G.I. Shapiro, G.S. Falchook, T.J. Price, A. Sacher, C.S. Denlinger, Y.J. Bang, G.K. Dy, J.C. Krauss, Y. Kuboki, J.C. Kuo, A.L. Coveler, K. Park, T.W. Kim, F. Barlesi, P.N. Munster, S.S. Ramalingam, T.F. Burns, F. Meric-Bernstam, H. Henary, J. Ngang, G. Ngarmchamnanrith, J. Kim, B.E. Houk, J. Canon, J.R. Lipford, G. Friberg, P. Lito, R. Govindan, B.T. Li, KRAS(G12C) inhibition with sotorasib in advanced solid tumors, N. Engl. J. Med. 383 (13) (2020) 1207–1217.
[32] S. Hyun, D. Shin, Small-molecule inhibitors and degraders targeting KRAS-driven cancers, Int. J. Mol. Sci. 22 (22) (2021).
[33] D. Grapsa, K. Syrigos, Direct KRAS inhibition: progress, challenges, and a glimpse into the future, Expert Rev. Anticancer Ther. 20 (6) (2020) 437–440.
[34] S.N. Mali, A. Pandey, R.R. Bhandare, A.B. Shaik, Identification of hydantoin based Decaprenylphosphoryl-beta-D-Ribose Oxidase (DprE1) inhibitors as antimycobacterial agents using computational tools, Sci. Rep. 12 (1) (2022) 16368.
[35] M.H. Baig, K. Ahmad, S. Roy, J.M. Ashraf, M. Adil, M.H. Siddiqui, S. Khan, M.A. Kamal, I. Provaznik, I. Choi, Computer aided drug design: success and limitations, Curr. Pharmaceut. Des. 22 (5) (2016) 572–581.
[36] D.B. Kitchen, H. Decornez, J.R. Furr, J. Bajorath, Docking and scoring in virtual screening for drug discovery: methods and applications, Nat. Rev. Drug Discov. 3 (11) (2004) 935–949.
[37] S.N. Mali, A. Pandey, Synthesis of new hydrazones using a biodegradable catalyst, their biological evaluations and molecular modeling studies (Part-II), Journal of Computational Biophysics and Chemistry 21 (7) (2022) 857–882.
[38] S.A. Hollingsworth, R.O. Dror, Molecular dynamics simulation for all, Neuron 99 (6) (2018) 1129–1143.
[39] X. Liu, D. Shi, S. Zhou, H. Liu, H. Liu, X. Yao, Molecular dynamics simulations and novel drug discovery, Expet Opin. Drug Discov. 13 (1) (2018) 23–37.
[40] D. Barh, V. Chaitankar, E.C. Yiannakopoulou, E.O. Salawu, S. Chowbina, P. Ghosh, V. Azevedo, In silico models: from simple networks to complex diseases, Anim. Biotechnol. (2014) 385–404. Elsevier.
[41] S. Salentin, V.J. Haupt, S. Daminelli, M. Schroeder, Polypharmacology rescored: protein-ligand interaction profiles for remote binding site similarity assessment, Prog. Biophys. Mol. Biol. 116 (2–3) (2014) 174–186.
[42] C. Zhu, X. Guan, X. Zhang, X. Luan, Z. Song, X. Cheng, W. Zhang, J.J. Qin, Targeting KRAS mutant cancers: from druggable therapy to drug resistance, Mol. Cancer 21 (1) (2022) 159.
[43] L. Herdeis, D. Gerlach, D.B. McConnell, D. Kessler, Stopping the beating heart of cancer: KRAS reviewed, Curr. Opin. Struct. Biol. 71 (2021) 136–147.
[44] Z. Zhang, K.Z. Guiley, K.M. Shokat, Chemical acylation of an acquired serine suppresses oncogenic signaling of K-Ras(G12S), Nat. Chem. Biol. 18 (11) (2022) 1177–1183.
[45] B.O. Herzberg, G.A. Manji, KRAS: druggable at last, Oncol. 28 (4) (2023) 283–286.
[46] W. Ning, Z. Yang, G.J. Kocher, P. Dorn, R.W. Peng, A breakthrough brought about by targeting KRAS(G12C): nonconformity is punished, Cancers 14 (2) (2022).
[47] Q. Zheng, D.M. Peacock, K.M. Shokat, Drugging the next undruggable KRAS allele-Gly12Asp, J. Med. Chem. 65 (4) (2022) 3119–3122.
[48] Z. Hu, J. Marti, Discovering and targeting dynamic drugging pockets of oncogenic proteins: the role of magnesium in conformational changes of the G12D mutated kirsten rat sarcoma-guanosine diphosphate complex, Int. J. Mol. Sci. 23 (22) (2022).
[49] D. Tang, R. Kang, Glimmers of hope for targeting oncogenic KRAS-G12D, Cancer Gene Ther. 30 (3) (2023) 391–393.
[50] H.A. Blair, Sotorasib: first approval, Drugs 81 (13) (2021) 1573–1579.
[51] S. Dhillon, Adagrasib: first approval, Drugs 83 (3) (2023) 275–285.